

Nonlinear hydrodynamic theory for a dilute gas-solid suspension

Saikat Saha^{1,*} and Meheboob Alam^{2,**}

¹Department of Mathematics, Indian Institute of Technology Roorkee, Roorkee-247667, India

²Engineering Mechanics Unit, Jawaharlal Nehru Centre for Advanced Scientific Research, Jakkur PO, Bengaluru 560064, India

Abstract. A second-order hydrodynamic theory is proposed for a dilute gas-solid suspension within the framework of the inelastic Boltzmann equation. A distribution function based on 14-hydrodynamic fields is used to calculate the collisional source terms that are correct up-to the second-order in hydrodynamic fields. This theory is used to analyse the uniform shear flow of a gas-solid suspension, yielding results on the granular temperature, the shear viscosity and the two normal stress differences. The theoretical results are compared with the predictions of the anisotropic Maxwellian theory (Saha & Alam, 2017, *J. Fluid Mech.*, vol. **833**, 206-246) and the particle simulation data over a range of Stokes numbers varying from order one to its dry granular limit. The inclusion of the second order nonlinearity in the collisional source term is found to be responsible for the non-zero second normal stress difference.

1 Introduction

A rapidly sheared granular gas, a collection of macroscopic solid particles in a fluidized state, mimics the classical picture of a molecular gas, and the methods from the kinetic theory [1] have been used to study and understand the hydrodynamics of a granular gas. Note that a fundamental difference between a molecular gas and a granular gas is that the grains collide inelastically and their kinetic energy is continually decreased unless it is replenished via external source such as shaking or shearing.

There exists an extensive body of works on the kinetic theory descriptions of rapid granular flows [2, 3] where the effect of the interstitial fluid is usually neglected (also called the “dry” granular fluid). The linearized version of Grad’s [4] 10 moment or 14 moment descriptions [2, 5, 6] can be cited as similar analyses. On the other hand, the effect of the interstitial gas on the momentum transport within the particle phase for a homogeneously sheared gas-solid suspension was first analysed by Tsao & Koch (1995) [7]; Saha & Alam (2017) [8] revisited the latter analysis using the anisotropic Maxwellian [9–11] approach that yielded excellent agreement with particle simulation results. Motivated by these works [8, 12–14], here we propose a second-order theory for a dilute gas-solid suspension under general deformation, and apply it to obtain the particle-phase rheological quantities in a uniform shear flow.

2 Nonlinear 14 moment theory

We propose a nonlinear 14 moment theory for a dilute gas solid suspension where identical, smooth, inelastic solid

particles (each having the mass m and diameter σ) are suspended in the bath of a Newtonian gas. The particles are undergoing interparticle inelastic collisions (with coefficient of inelasticity e), and experience a viscous drag where it is assumed that the particle inertia (the Stokes number $St = \dot{\gamma}\tau_v \gg 1$, $\dot{\gamma}$ is the overall shear rate and τ_v is the viscous relaxation time of the particles) dominates over the fluid inertia (the Reynolds number $Re = \rho_{\text{gas}}\dot{\gamma}\sigma^2/\mu_{\text{gas}} \ll 1$). The gas-phase is a continuum and its velocity \mathbf{v} follows the Stokes equations of motion. We are interested in the particle phase momentum transport and employ the relevant kinetic theory [1] that holds for a dilute granular gas. The single particle velocity distribution function $f^{(1)}(\mathbf{c}, \mathbf{x}, t)$ is governed the celebrated Boltzmann equation [7]

$$\left(\frac{\partial}{\partial t} + \mathbf{c} \cdot \nabla_{\mathbf{x}}\right) f^{(1)} + \nabla_{\mathbf{c}} \cdot \left(f^{(1)} \frac{d\mathbf{c}}{dt}\right) = \left(\frac{\partial f^{(1)}}{\partial t}\right)_{\text{coll}}, \quad (1)$$

where $\left(\frac{\partial f^{(1)}}{\partial t}\right)_{\text{coll}}$ is the collision operator and the divergence term in the left hand side includes the gas effects.

2.1 Fourteen field variables

The conversion from the particle level to the hydrodynamic level is done by taking appropriate moments with respect to the single particle distribution function $f^{(1)}(\mathbf{c}, \mathbf{x}, t)$ and we assume that the macroscopic state of the particle phase is characterized by 14 hydrodynamic-like fields: (i) the mass density

$$\rho(\mathbf{x}, t) \equiv mn(\mathbf{x}, t) = m \int f^{(1)}(\mathbf{c}, \mathbf{x}, t) d\mathbf{c}, \quad (2)$$

(ii) the macroscopic flow velocity

$$\mathbf{u}(\mathbf{x}, t) \equiv \langle \mathbf{c} \rangle = \frac{1}{n} \int \mathbf{c} f^{(1)} d\mathbf{c}, \quad (3)$$

*e-mail: saikat.saha@ma.iitr.ac.in

**e-mail: meheboob@jncasr.ac.in

(iii) the full second moment tensor

$$\mathbf{M}(\mathbf{x}, t) \equiv \langle \mathbf{C}\mathbf{C} \rangle = \frac{1}{n} \int \mathbf{C}\mathbf{C} f^{(1)} d\mathbf{C}, \quad (4)$$

where $\mathbf{C} = \mathbf{c} - \mathbf{u}$ is the fluctuation velocity. (iv) The heat flux vector is defined as

$$\mathbf{q}(\mathbf{x}, t) \equiv \frac{1}{2} \rho \langle \mathbf{C}^2 \mathbf{C} \rangle = \frac{m}{2} \int \mathbf{C}^2 \mathbf{C} f^{(1)} d\mathbf{C}, \quad (5)$$

and (v) the excess kurtosis $\alpha_2 = (P_{\alpha\alpha\beta\beta} - P_{\alpha\alpha\beta\beta}^M) / P_{\alpha\alpha\beta\beta}^M$, where $P_{\alpha\alpha\beta\beta}$ is the fully contracted fourth moment

$$P_{\alpha\alpha\beta\beta}(\mathbf{x}, t) \equiv \rho \langle \mathbf{C}^4 \rangle = m \int \mathbf{C}^4 f^{(1)} d\mathbf{C}, \quad (6)$$

and $P_{\alpha\alpha\beta\beta}^M$ is its Maxwellian counterpart. The granular temperature is defined as the trace of the second moment tensor \mathbf{M} , and the stress tensor is defined as $\mathbf{P} = \rho \mathbf{M} \equiv p \mathbf{I} + \mathbf{\Pi}$, where p is the pressure and $\mathbf{\Pi}$ is the stress deviator.

2.2 Balance equations for fourteen field variables

The balance equations for the fourteen field variables [(2-6)] are obtained from (1) as listed below:

$$\frac{D\rho}{Dt} = -\rho u_{\alpha,\alpha}, \quad (7)$$

$$\rho \frac{Du_\alpha}{Dt} = -P_{\alpha\beta,\beta} - \frac{\dot{\gamma}}{St} \rho (u_\alpha - v_\alpha), \quad (8)$$

$$\frac{DP_{\alpha\beta}}{Dt} = -Q_{\gamma\alpha\beta,\gamma} - P_{\alpha\beta} u_{\alpha,\alpha} - P_{\delta\beta} u_{\alpha,\delta} - P_{\delta\alpha} u_{\beta,\delta} - \frac{2\dot{\gamma}}{St} P_{\alpha\beta} + \mathfrak{N}_{\alpha\beta}, \quad (9)$$

$$\frac{Dq_\alpha}{Dt} = -\frac{1}{2} Q_{\gamma\alpha\beta\beta,\gamma} - q_\alpha u_{\delta,\delta} - q_\beta u_{\alpha,\beta} - Q_{\gamma\alpha\beta} u_{\beta,\gamma} + \frac{1}{\rho} \left(P_{\alpha\beta} + \frac{1}{2} P_{\gamma\gamma} \delta_{\alpha\beta} \right) P_{\beta n,n} - \frac{3\dot{\gamma}}{St} q_\alpha + \frac{1}{2} \mathfrak{N}_{\alpha\beta\beta}, \quad (10)$$

$$15\rho T^2 \frac{D\alpha_2}{Dt} = -8T \left(1 - \frac{5}{2} \alpha_2 \right) (q_{\alpha,\alpha} + P_{(\alpha\beta)} u_{\beta,\alpha}) + \frac{8q_\alpha}{\rho} \left(T \frac{\partial \rho}{\partial x_\alpha} + \frac{\partial P_{(\alpha\beta)}}{\partial x_\beta} \right) - 20q_\alpha \frac{\partial T}{\partial x_\alpha} + \mathfrak{N}_{\alpha\alpha\beta\beta} - 10T (1 + \alpha_2) \mathfrak{N}_{\alpha\alpha}, \quad (11)$$

where the underlined terms in (7)-(11) are the contributions from the gas phase and identifies the viscous contribution to the particle phase. $\mathfrak{N}_{\alpha\beta}$, $\mathfrak{N}_{\alpha\beta\beta}$, $\mathfrak{N}_{\alpha\alpha\beta\beta}$, are the collisional sources of the second, third and fourth moments, respectively, and $Q_{\alpha\beta\gamma\dots} = \rho \langle C_\alpha C_\beta \dots C_\gamma \rangle$.

In order to obtain a complete 14-moment theory, all collisional source terms must be calculated by an appropriate choice of the single-particle distribution function.

2.3 Non-equilibrium distribution function

Following Grad [4], we assume that the non-equilibrium distribution function is an expansion around the Maxwellian in terms of the fourteen hydrodynamic

fields. By satisfying the compatibility conditions (2-6), the distribution function is obtained as

$$f^{(1)} = \frac{n}{(2\pi T)^{3/2}} \exp(-C^2/2T) \left\{ 1 + \frac{1}{2\rho T^2} P_{(ij)} C_i C_j + \frac{q_i}{5\rho T^3} (C^2 C_i - 5T C_i) + \alpha_2 \left(\frac{15}{8} - \frac{5C^2}{4T} + \frac{C^4}{8T^2} \right) \right\}. \quad (12)$$

2.4 Collisional source terms

The collisional source terms in the moment balances (9)-(11) have been calculated using the above form of the distribution function (12). For the sake of brevity, we are writing the most important term, namely, the collisional source of the second moment which is correct up-to second-order in hydrodynamic fields:

$$\begin{aligned} \mathfrak{N}_{\alpha\beta} = & -\frac{(1+e)\rho v g_0 T^{\frac{3}{2}}}{64\sqrt{\pi}\sigma} \left[\frac{1}{2} (1-e) (32 + 3\alpha_2)^2 \delta_{\alpha\beta} + \frac{48}{5} (3-e) \right. \\ & \times (32 - \alpha_2) \frac{\Pi_{\alpha\beta}}{\rho T} + \frac{64}{35\rho^2 T^2} \left\{ 12(3-e) \Pi_{\alpha l} \Pi_{l\beta} - (5+3e) \Pi_{lk} \Pi_{lk} \delta_{\alpha\beta} \right\} \\ & + \frac{64}{125\rho^2 T^3} \left\{ 6(3-e) q_\alpha^{(k)} q_\beta^{(k)} - (1+3e) q_l^{(k)} q_l^{(k)} \delta_{\alpha\beta} \right\} \left. \right] \\ & - \frac{2(1+e)v g_0}{175} \left[\frac{7}{\rho} \left\{ 3(2-e) (q_\alpha \rho_\beta + q_\beta \rho_\alpha) + (1-3e) q_{k\rho,k} \delta_{\alpha\beta} \right\} \right. \\ & - 35\rho T \left\{ 3(2-e) (u_{\alpha,\beta} + u_{\beta,\alpha}) + (1-3e) u_{k,k} \right\} \\ & - 10 \left\{ (11-3e) (\Pi_{\alpha k} u_{\beta,k} + \Pi_{\beta k} u_{\alpha,k} + \Pi_{\alpha\beta} u_{k,k}) \right. \\ & + (4-3e) (\Pi_{\alpha k} u_{k,\beta} + \Pi_{\beta k} u_{k,\alpha}) - 3(1+e) \Pi_{kl} u_{k,l} \delta_{\alpha\beta} \left. \right\} \\ & \left. - 7 \left\{ 3(2-e) (q_{\alpha,\beta} + q_{\beta,\alpha}) + (1-3e) q_{k,k} \delta_{\alpha\beta} \right\} \right] \\ & - \frac{(1+e)v\sigma}{177408\sqrt{\pi}\rho T^{3/2}} \left[99\rho^2 T^2 [(1024-64\alpha_2-1935\alpha_2^2)\{2(13-3e)u_{\alpha,k}u_{\beta,k} \right. \\ & - (1+3e)\delta_{\alpha\beta}(u_{k,l}u_{l,k} + u_{k,k}u_{l,l}) + 6(2-e)(u_{\alpha,k}u_{k,\beta} + u_{k,k}u_{\alpha,\beta}) \\ & + 6(2-e)(u_{\beta,k}u_{k,\alpha} + u_{k,k}u_{\beta,\alpha}) - \{(1+3e)(1024-64\alpha_2) \\ & + 15(1663-2179e)\alpha_2^2\}(\delta_{\alpha\beta}u_{k,l}u_{k,l} + 2u_{k,\alpha}u_{k,\beta})] \\ & - 352(32+3\alpha_2)\rho T [(5+3e)\Pi_{kl}\{\delta_{\alpha\beta}u_{k,l}u_{l,i} + 2u_{k,\alpha}u_{l,\beta} \\ & + \delta_{\alpha\beta}(u_{i,k}u_{i,l} + 2u_{k,i}u_{l,i} + 2u_{i,i}u_{k,l})\} \\ & - 2(4-3e)\{\Pi_{k\alpha}(u_{l,k}u_{l,\beta} + u_{k,l}u_{l,\beta} + u_{k,\beta}u_{l,l}) + \Pi_{kl}(u_{\alpha,k}u_{l,\beta} + u_{k,l}u_{\alpha,\beta})\} \\ & - 2(4-3e)\{\Pi_{k\beta}(u_{l,k}u_{l,\alpha} + u_{k,l}u_{l,\alpha} + u_{k,\alpha}u_{l,l}) + \Pi_{kl}(u_{\beta,k}u_{l,\alpha} + u_{k,l}u_{\beta,\alpha})\} \\ & - (13-3e)\{2\Pi_{\alpha k}(u_{k,l}u_{\beta,l} + u_{l,k}u_{\beta,l} + u_{\beta,k}u_{l,l}) + 2\Pi_{\beta k}(u_{k,l}u_{\alpha,l} + u_{l,k}u_{\alpha,l}) \\ & + u_{\alpha,k}u_{l,l} + 2\Pi_{kl}u_{\alpha,k}u_{\beta,l} + \Pi_{\alpha\beta}(u_{k,l}u_{k,l} + u_{k,l}u_{l,k} + u_{k,k}u_{l,l})\} \\ & + 384(3+e)[\Pi_{ij}\Pi_{ij}\{2u_{k,\alpha}u_{k,\beta} + \delta_{\alpha\beta}(u_{k,l}u_{k,l} + u_{k,l}u_{l,k} + u_{k,k}u_{l,l})\} \\ & + 4\Pi_{ik}\Pi_{il}\{2u_{k,\alpha}u_{l,\beta} + \delta_{\alpha\beta}(u_{k,j}u_{l,j} + u_{j,k}u_{j,l})\} \\ & + 4\delta_{\alpha\beta}\Pi_{ij}\Pi_{kl}(u_{i,j}u_{k,l} + u_{i,k}u_{j,l} + u_{k,i}u_{j,l})] \\ & - 256(13-3e)[\Pi_{ij}\Pi_{ij}u_{\alpha,k}u_{\beta,k} + 4\Pi_{ik}\Pi_{il}u_{\alpha,k}u_{\beta,l} \\ & + 2\Pi_{i\alpha}\Pi_{i\beta}(u_{k,l}u_{k,l} + u_{k,l}u_{l,k} + u_{k,k}u_{l,l}) \\ & + 4\Pi_{k\alpha}\Pi_{i\beta}(u_{k,i}u_{l,i} + u_{i,k}u_{i,l} + u_{k,l}u_{i,i} + u_{l,k}u_{i,i} + u_{i,l}u_{k,i}) \\ & + 2\Pi_{kl}\Pi_{\alpha\beta}(u_{k,i}u_{l,i} + u_{i,k}u_{i,l} + 2u_{k,l}u_{i,i} + 2u_{k,i}u_{l,i}) + 4\Pi_{ik}\Pi_{i\alpha}u_{k,l}u_{\beta,l} \\ & + 4\Pi_{k\alpha}\Pi_{kl}(u_{\beta,l}u_{i,i} + u_{i,l}u_{\beta,i}) + 4\Pi_{i\alpha}\Pi_{kl}(u_{\beta,i}u_{k,l} + u_{i,k}u_{\beta,l} + u_{k,i}u_{\beta,l}) \\ & + 4\Pi_{ik}\Pi_{i\beta}u_{k,l}u_{\alpha,l} + 4\Pi_{k\beta}\Pi_{kl}(u_{\alpha,l}u_{i,i} + u_{i,l}u_{\alpha,i}) \\ & \left. + 4\Pi_{i\beta}\Pi_{kl}(u_{\alpha,i}u_{k,l} + u_{i,k}u_{\alpha,l} + u_{k,i}u_{\alpha,l}) \right] \quad (13) \end{aligned}$$

$$\begin{aligned}
 & -256(2-3e)[\Pi_{ij}\Pi_{ij}(u_{\alpha,k}u_{k,\beta} + u_{k,k}u_{\alpha,\beta}) + 4\Pi_{ik}\Pi_{i\alpha}u_{l,k}u_{l,\beta} \\
 & + 4\Pi_{ik}\Pi_{il}(u_{k,l}u_{\alpha,\beta} + u_{\alpha,k}u_{l,\beta}) + 4\Pi_{k\alpha}\Pi_{kl}(u_{l,\beta}u_{i,i} + u_{i,\beta}u_{l,i}) \\
 & \quad + 4\Pi_{i\alpha}\Pi_{kl}(u_{i,\beta}u_{k,l} + u_{k,i}u_{l,\beta} + u_{i,k}u_{l,\beta}) \\
 & \quad + \Pi_{ij}\Pi_{ij}(u_{\beta,k}u_{k,\alpha} + u_{k,k}u_{\beta,\alpha}) + 4\Pi_{ik}\Pi_{i\beta}u_{l,k}u_{l,\alpha} \\
 & + 4\Pi_{ik}\Pi_{il}(u_{k,l}u_{\beta,\alpha} + u_{\beta,k}u_{l,\alpha}) + 4\Pi_{k\beta}\Pi_{kl}(u_{l,\alpha}u_{i,i} + u_{i,\alpha}u_{l,i}) \\
 & \quad + 4\Pi_{i\beta}\Pi_{kl}(u_{i,\alpha}u_{k,l} + u_{k,i}u_{l,\alpha} + u_{i,k}u_{l,\alpha})] \\
 & + \frac{4224}{25T} [(5+3e)[q_k q_k \{\delta_{\alpha\beta}(u_{l,i}u_{l,i} + u_{l,i}u_{i,l} + u_{l,i}u_{i,i}) + 2u_{l,\alpha}u_{l,\beta}\} \\
 & + 2q_k q_l \{\delta_{\alpha\beta}(u_{i,k}u_{i,l} + u_{k,i}u_{l,i} + 2u_{i,k}u_{l,i} + 2u_{k,l}u_{i,i}) + 2u_{k,\alpha}u_{l,\beta}\}] \\
 & \quad - 2(13-3e)[q_k q_k u_{\alpha,l}u_{\beta,l} + 2q_k q_l u_{\alpha,k}u_{\beta,l} \\
 & + q_\alpha q_\beta (u_{k,l}u_{k,l} + u_{k,l}u_{l,k} + u_{k,k}u_{l,l}) + 2q_k q_\alpha (u_{\beta,l}u_{k,l} + u_{\beta,l}u_{l,k} + u_{\beta,k}u_{l,l}) \\
 & \quad + 2q_k q_\beta (u_{\alpha,l}u_{k,l} + u_{\alpha,l}u_{l,k} + u_{\alpha,k}u_{l,l}) \\
 & - 2(4-3e)[q_k q_k (u_{\alpha,l}u_{l,\beta} + u_{l,l}u_{\alpha,\beta}) + 2q_k q_l (u_{\alpha,k}u_{l,\beta} + u_{k,l}u_{\alpha,\beta}) \\
 & + 2q_k q_\alpha (u_{k,l}u_{l,\beta} + u_{l,k}u_{l,\beta} + u_{k,\beta}u_{l,l}) + q_k q_k (u_{\beta,l}u_{l,\alpha} + u_{l,l}u_{\beta,\alpha}) \\
 & + 2q_k q_l (u_{\beta,k}u_{l,\alpha} + u_{k,l}u_{\beta,\alpha}) + 2q_k q_\beta (u_{k,l}u_{l,\alpha} + u_{l,k}u_{l,\alpha} + u_{k,\alpha}u_{l,l})]] \\
 & + \text{terms proportional to } \{\nabla\rho\nabla\rho, \nabla\rho\nabla T, \dots \nabla\alpha_2\nabla\alpha_2\}.
 \end{aligned}$$

3 Results and discussion

3.1 Uniform shear flow

As an application of the above theory, we calculate the particle phase stress tensor in a gas-solid suspension under the steady shearing state. The macroscopic particle phase velocity for a simple shear flow is given by $\mathbf{u} = \mathbf{v} = \dot{\gamma}y\hat{e}_x$. In this class of flows, the shear work is exactly balanced by (i) the viscous drag and (ii) the inelastic dissipation, and under this flow situation, the balance of mass (7) and momentum (8) get trivially satisfied whereas the second moment balance (9) simplified into

$$P_{\delta\beta}u_{\alpha,\delta} + P_{\delta\alpha}u_{\beta,\delta} + \frac{2\dot{\gamma}}{St}P_{\alpha\beta} = \mathfrak{N}_{\alpha\beta}. \quad (14)$$

Equation (14) must be solved with the aid of (13) to determine the complete stress tensor \mathbf{P} .

3.2 Shear viscosity and normal stress differences

We normalize the stress tensor via

$$P_{\alpha\beta}^* = \frac{P_{\alpha\beta}}{\rho(\dot{\gamma}\sigma/2)^2} = T^* + P_{\langle\alpha\beta\rangle}^*, \quad (15)$$

where $T^* = T/(\dot{\gamma}\sigma/2)^2$ is the dimensionless granular temperature, $\mu^* = -P_{xy}/\rho(\dot{\gamma}\sigma/2)^2$ is the dimensionless shear viscosity, and the first and second normal stress differences are given by $\mathcal{N}_1 = 3(P_{xx} - P_{yy})/(P_{xx} + P_{yy} + P_{zz})$, $\mathcal{N}_2 = 3(P_{yy} - P_{zz})/(P_{xx} + P_{yy} + P_{zz})$, respectively. For convenience, we will be denoting the dimensionless temperature and shear viscosity by T and μ , respectively, from here onwards.

Figure 1 displays the variations of (a) the granular temperature and (b) the particle phase shear viscosity against the Stokes inverse (St^{-1}) for a coefficient of restitution $e = 0.9$ and a particle volume fraction of $\phi = 0.01$. It is observed that the temperature decays with (St^{-1}). This

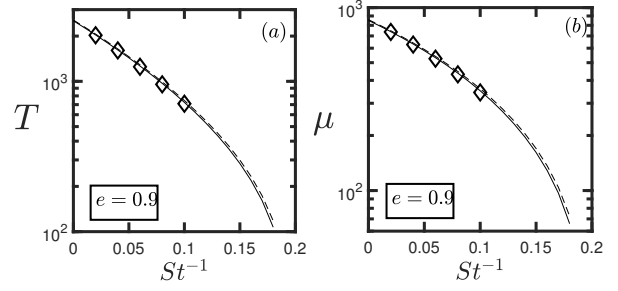


Figure 1. Variations of (a) the granular temperature (T) and (b) the particle phase shear viscosity μ against the inverse of Stokes number (St^{-1}) at coefficient of restitution $e = 0.9$. The continuous lines represent the predictions from the present nonlinear theory, the dashed lines represent the anisotropic Gaussian theory of Saha & Alam (2017) [8] and open diamonds represent the DSMC results.

behaviour of T can be explained from the fact that Stokes number ($St = \dot{\gamma}\tau_v$) increases with the viscous relaxation time τ_v , and an increasing τ_v simply means that the particles cover more distances between collisions, leading to a lesser collisional frequency which finally reflects as a higher temperature with increasing St . The similar behaviour of the shear viscosity μ follows from the fact that, in the dilute limit, shear viscosity scales like \sqrt{T} . Finally, for a comparison, the DSMC [15] predicted values and the results from the anisotropic Maxwellian theory [8, 13] are superimposed, and an excellent agreement among the present theory, the anisotropic Maxwellian theory [8], and the simulation is observed. The results of the present nonlinear Grad moment expansion (GME) and the anisotropic Maxwellian expansion (AME) are almost indistinguishable upto $St \sim 10$.

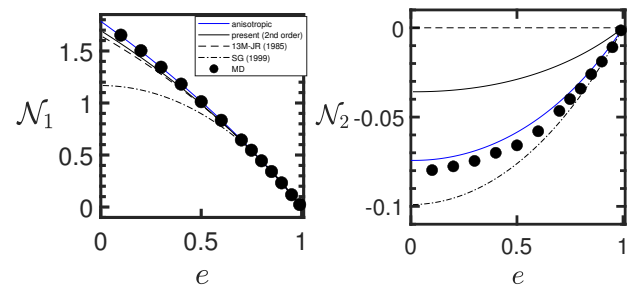


Figure 2. Variations of the first (\mathcal{N}_1) and second (\mathcal{N}_2) normal stress differences with e for a dry granular gas ($St \rightarrow \infty$). The legend in left panel explains the meaning of different lines and symbols.

Figure 2 describes how the first (\mathcal{N}_1) and second (\mathcal{N}_2) normal stress differences [16, 17] vary with inelasticity (e) for a dry granular fluid ($St \rightarrow \infty$). It compares the results obtained from several existing Grad-level and anisotropic Gaussian theories. The dashed and dot-dashed lines represent the predictions from the Grad-13 moment theory [2, 6] and the Burnett order Chapman-Enskog expansion [3], respectively, whereas the solid lines represent the predictions from the present nonlinear 10/14-moment the-

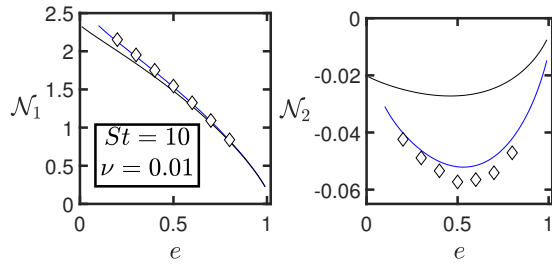


Figure 3. Same as Fig. 2, but for a suspension at $St = 10$.

ory. Finally, the solid blue lines represent the anisotropic Maxwellian theory [8] and the filled circles represent the molecular-dynamics simulation data [16]. The variations of the two normal stress differences with inelasticity for a suspension having significant viscous effects ($St = 10$) are shown in figure (3). The present theory over-predicts N_2 , but it can be noticed that, at this value of Stokes ($St = 10$), the overall magnitude of N_2 is indeed small. On the other hand, the predictions for N_1 remain spot on.

In rapid granular shear flows, both the normal stress differences are known to increase in magnitude with increasing dissipation [3, 16, 17]; both normal stresses scale like $\dot{\gamma}^2$ (and hence a Burnett-order effect) where we have $\dot{\gamma} \sim \sqrt{1-e}$ for a dilute granular gas ($e \neq 1$). It can be seen from Fig. 2 (left panel) that the Chapman-Enskog solution [3] (dot-dashed lines) for N_1 quantitatively matches with simulation upto $e = 0.5$, with increasing deviations at $e < 0.5$, and it mostly underpredicts N_2 . On the other hand, the “linearized” Grad-13 moment theory [2, 5, 6] (dashed lines) quantitatively agrees well with the simulation for N_1 , however, it predicts $N_2 = 0$ which turns out to be a major short-coming of the “linearized” Grad-moment theory. We find in Figs. 2 and 3 (right panels) that the same Grad-moment expansion but with added nonlinearity yields a non-zero second normal stress difference (solid line) which agrees qualitatively with the particle simulation data. It can also be seen in Fig. 2 that the prediction for N_1 becomes better with our second-order theory. On the other hand, the quantitative agreement for N_2 is much better (both for dry granular and gas-solid suspension) with the anisotropic Maxwellian theory [8] due to the non-perturbative nature of the latter approach. The related issues, along with the roles of frictional particles and a turbulent gas on the present theory, will be discussed at the conference.

4 Conclusion and outlook

We have proposed a nonlinear 14 moment theory for a dilute gas-solid suspension undergoing general deformation. The particle phase dynamics is governed by the inelastic Boltzmann equation that includes the viscous gas effects. This theory is applied to analyse the simple shear flow

of a gas-solid suspension. It is observed that the granular temperature, shear viscosity, and the first normal stress difference agree well with the particle simulation results, and the agreement remains excellent even for large dissipations ($e \sim 0$). We have predicted a non-zero second normal stress difference that agrees qualitatively with simulation results, and the origin of the non-zero second normal stress difference in the present theory is tied to the inclusion of nonlinear terms.

The solution we have analysed in this paper so far is an ignited state description where the granular temperature is large: the present theory can be modified by taking into account the quenched state contribution to the collisional source term [7] to probe the existence of a low temperature quenched state. Finally, the collisional contributions to the stress tensor can be calculated to obtain the normal stress differences for a dense suspension [12, 14] at any Stokes number ($1 < St < \infty$).

Acknowledgement

S.S. is supported by the SERB, Govt. of India under the Startup Research Grant (file number SRG/2023/002697).

References

- [1] S. Chapman, T. Cowling, *The Mathematical Theory of Non-uniform Gases* (Cambridge University Press, Cambridge, 1970)
- [2] J.T. Jenkins, M.W. Richman, *Arch. Rat. Mech. Anal.* **87**, 355 (1985).
- [3] N. Sela, I. Goldhirsch, *J. Fluid Mech.* **361**, 41 (1998).
- [4] H. Grad, *Commun. Pure & App. Math.* **2**, 79 (1949).
- [5] G.M. Kremer, M. Wilson, *Kinetic and Related Models* **4**, 317-331 (2011).
- [6] V. Garzo, *Phys. Fluids* **25**, 043301 (2013).
- [7] H.-K. Tsao, D.L. Koch, *J. Fluid Mech.* **296**, 211 (1995).
- [8] S. Saha, M. Alam, *J. Fluid Mech.* **833**, 206 (2017).
- [9] J.T. Jenkins, M.W. Richman, *J. Fluid Mech.* **192**, 313 (1988).
- [10] S. Saha, M. Alam, *J. Fluid Mech.* **757**, 251 (2014).
- [11] S. Saha, M. Alam, *J. Fluid Mech.* **795**, 549 (2016).
- [12] M. Alam, S. Saha, *EPJ Web Conf.* **140**, 11014 (2017).
- [13] M. Alam, S. Saha, R. Gupta, *J. Fluid Mech.* **870**, 1175 (2019).
- [14] S. Saha, M. Alam, *J. Fluid Mech.* **887**, A9 (2020).
- [15] R. Gupta, M. Alam, *Phys. Rev. E* **95**, 022903 (2017).
- [16] M. Alam, S. Luding, *Powders and Grains* (Eds: R. Garcia-Rojo, H.J. Herrmann & S. McNamara; A. A. Balkema, Netherlands), 1141-1145 (2005).
- [17] M. Alam, S. Luding, *Phys. Fluids.* **15**, 2298-2312 (2005).